

The nonlinear response of a quantum dot in a time-dependent field

This article has been downloaded from IOPscience. Please scroll down to see the full text article.

1996 J. Phys.: Condens. Matter 8 3427

(<http://iopscience.iop.org/0953-8984/8/19/018>)

[View the table of contents for this issue](#), or go to the [journal homepage](#) for more

Download details:

IP Address: 171.66.16.208

The article was downloaded on 13/05/2010 at 16:38

Please note that [terms and conditions apply](#).

The nonlinear response of a quantum dot in a time-dependent field

Tzanko Ivanov

Department of Physics, University of Sofia, 1126 Sofia, Bulgaria

Received 7 November 1995, in final form 5 February 1996

Abstract. We calculate the rectification coefficient a_{rect} and the second-harmonic generation coefficient $a_{2\Omega}$ for a quantum dot biased with an ac field. The coefficients are calculated as functions of the gate voltage (i.e. the positions of the resonant levels) and the frequency of the applied field. The rectification coefficient has a peaked dependence on the gate voltage with one central (negative) and two side (positive) peaks around the voltage at which the corresponding energy level for interacting electrons is equal to the collector electrode chemical potential. The peak heights are related to the average number of electrons in the dot—a feature which is a direct consequence of the electron interactions. The second-harmonic generation coefficient has similar behaviour for low frequencies ($a_{rect} = a_{2\Omega}$ at zero frequency). The frequency dependence of the rectification coefficient has features resulting from the photon-assisted tunnelling through the dot. The resonant-like enhancement of the rectification coefficient cannot be attributed to the photon-assisted transitions between different resonant levels in the dot.

1. Introduction

Recently, the transport through resonant tunnelling systems in time-dependent fields has been attracting much interest. Quantum dots are among the simplest systems for which to study the time-dependent dynamics of nonequilibrium states, with possible applications in high-speed electronics. The extremely fast response of double-barrier resonant tunnelling structures (DBRTS) to an applied field has been demonstrated in picosecond switches [1] and high-frequency negative-resistance oscillations [2, 3]. Comparison of the high-frequency current response and the static I – V characteristic showed that the charge-transport response time is less than 10^{-13} s [4].

Various approaches have been adopted to study the transport through a quantum dot in time-dependent fields—linear response calculations [5–7], non-Markovian master equations [8], and nonlinear responses [9, 10]. In a Wigner function approach Frensky [9] calculated the nonlinear response coefficients (the rectification coefficient and the second-harmonic generation coefficient) and obtained a resonant enhancement of the rectification coefficient a_{rect} in the frequency range from 1 to 8 THz. In a transmission coefficient approach Wingreen [10] concluded that a_{rect} is determined by the dc I – V characteristic. He found that a_{rect} is a decreasing function of the frequency of the external field. We must point out that this result is in disagreement with both the results of Frensky [9] and the findings of the present work. Recently, Chitta *et al* [11] reported measurements of the far-infrared response of a quantum dot at frequencies up to 3.3 THz. On the basis of a coherent picture of the resonant tunnelling they concluded that the classical rectification cannot explain the

measured quantum well response. All of these theoretical investigations studied the response of a quantum dot without considering the electron-electron interactions.

In the present work we calculate the nonlinear response coefficients of a double-barrier resonant tunnelling system explicitly taking into account the effect of the Coulomb charging energy—the energy of the Coulomb repulsion between two electrons with opposite spins—on the resonant level of the quantum dot. Since we study quantum wells out of equilibrium (with an applied dc voltage) we employ the Keldysh Green's function technique [12, 13]. The electron distribution in the dot is calculated from the Keldysh distribution function in the presence of just the dc voltage. The expressions for the nonlinear response coefficients are derived in terms of the quantum dot electron Green's functions. We discuss their behaviour, comparing the cases of interacting and noninteracting electrons.

The paper is organized in the following way. In section 2 we formulate the model Hamiltonian of the quantum dot and introduce the nonequilibrium electron Green's functions in the Keldysh approach. In section 3 we derive the explicit expressions for the nonlinear response coefficients in terms of the electron Green's functions. In section 4 we discuss the behaviour of the nonlinear response coefficients in the case of two degenerate resonant levels in the dot. In the last section we comment on the applicability of our approach to experiments.

2. The quantum dot Hamiltonian and electron Green's functions

The starting point of our discussion is the Hamiltonian of the dot, coupled to two leads, which are considered as ideal reservoirs. The Anderson Hamiltonian is given by

$$H = \sum_{k,i=L,R} \epsilon_{ik} a_{ik}^\dagger a_{ik} + \sum_m \epsilon_m c_m^\dagger c_m + E_c \sum_{m,m':m \neq m'} n_m n_{m'} + \sum_{k,m,i=L,R} (T_{imk} c_m^\dagger a_{ik} + \text{HC}). \quad (1)$$

It is expressed in terms of the annihilation operators $c_m, a_{ik}, i = L, R$, for electrons in the well and quasiparticles in the left-hand ($i = L$) and the right-hand ($i = R$) lead, respectively. The quasiparticle energies $\epsilon_{ik}, i = L, R$, are measured from the corresponding Fermi levels μ_L and μ_R in the emitter ($i = L$) and collector ($i = R$), and the dc bias is $\mu_L - \mu_R = eV$. In the following we set $\mu_R = 0$. The index m runs over the dot energy levels as determined by the quantum confinement, and E_c is the Coulomb repulsion energy for repulsion between electrons on different energy levels ϵ_m and $\epsilon_{m'} (m \neq m')$. In the summation over m in equation (1) we include the possibility of degenerate energy levels. The particle number operator is $n_m = c_m^\dagger c_m$. In equation (1) $T_{imk}, i = L, R$, are the tunnelling matrix elements.

In writing this form of the Hamiltonian we make the following assumption: if some lowest-lying states in the dot are always occupied, they are excluded from the summation over m in equation (1). The electrons on these levels will modify (through the Coulomb interaction energy) the energies of the electrons on dot levels retained in equation (1). If, for example, there are N electrons in the lowest states, then

$$\epsilon_m = \epsilon_m^{(0)} + N E_c - e \frac{C_G V_G + C_L V}{C_\Sigma} \quad (2)$$

where $\epsilon_m^{(0)}$ is the bare resonant level energy, determined by the quantum confinement, and the last term describes the dependence of the resonant level energy on the applied gate and transport voltages (see figure 1 where the effective circuit of the dot is shown). The total capacitance of the dot is $C_\Sigma = C_L + C_R + C_G$ with $C_{L(R)}$ the capacitances of the left-hand

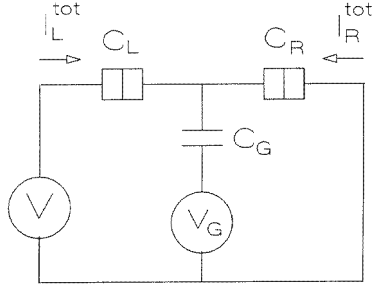


Figure 1. The effective circuit of the quantum dot.

(right-hand) electrode and C_G the gate electrode capacitance. The case of noninteracting electrons studied later in the text is obtained by putting $E_c = 0$.

We consider external time-dependent perturbation with a Hamiltonian given by

$$H_{ext} = -e \frac{C_G}{C_\Sigma} u(t) \sum_m c_m^\dagger(t) c_m(t) \quad (3)$$

where the external ac bias applied to the quantum well through the gate electrode is taken in the form

$$u(t) = u_0 \exp(i\Omega t) + \text{CC.} \quad (4)$$

Note that throughout the remainder of this paper (unless explicitly written) we have omitted Planck's constant \hbar .

Now let us introduce the Keldysh Green's functions of the quantum well electrons. There are three types of Green's function (GF) in the Keldysh formulation: the retarded (advanced) and the distribution functions [13]. The retarded GF is defined as

$$G_{mm'r}(t) = -i\theta(t) \langle \{c_m(t), c_{m'}^\dagger(0)\} \rangle \quad (5)$$

and the distribution function is

$$G_{mm'<}(t_1, t_2) = i \langle c_{m'}^\dagger(t_2) c_m(t_1) \rangle. \quad (6)$$

We recall that in the Keldysh technique the distribution GF depends on two times—the ‘relative’ time $t = t_1 - t_2$ and the ‘centre-of-mass’ time $T = (t_1 + t_2)/2$ —while the retarded GF depends only on a single time variable.

We do not give the details of the derivation of the Green's function, part of which can be found in [14]. We present only the final form of the retarded (advanced) and the distribution GF in some simple cases since the explicit expressions are too cumbersome to quote here.

3. Nonlinear response coefficients

In this section we derive the general formulas for the rectification coefficient and the second-harmonic generation coefficient. The tunnelling current through the left/right-hand barrier of the dot is given by

$$I_{L/R}(t) = -ie \left\langle \sum_{k,m} \left(T_{L/Rmk} c_m^\dagger(t) a_{L/Rk}(t) - \text{HC} \right) \tilde{S}(t) \right\rangle \quad (7)$$

where

$$\tilde{S}(t) = \tilde{T}_p \exp \left[-i \int_p dt' H_{ext}(t') \right].$$

\tilde{T}_p is the closed-path time-ordering operator [12] and the brackets in equation (7) denote averaging with respect to the Hamiltonian (1). The total current through the left/right-hand barrier of the dot is (see figure 1)

$$I_{L/R}^{tot} = \tilde{I}_{L/R} + \frac{C_{R/L} + C_G}{C_\Sigma} I_{L/R} - \frac{C_{L/R}}{C_\Sigma} I_{R/L} \quad (8)$$

where $\tilde{I}_{L/R}$ are the displacement currents through the parasitic capacitances. They are linear in the amplitude of the applied ac bias and do not contribute to the nonlinear response of the dot.

The nonlinear response coefficients are calculated by expanding the current equation (7) in powers of the external ac voltage bias $u(t)$. The term quadratic in the amplitude u_0 is given by

$$I_i^{II}(t) = \frac{ie^3}{2} \alpha^2 \left\langle \tilde{T}_p \int dt' \int dt'' u(t') u(t'') \sum_{k,m} \left(T_{imk} c_m^\dagger(t) a_{ik}(t) - \text{HC} \right)_+ \right. \\ \left. \times \left(\sum_{m'} c_{m'}^\dagger(t') c_{m'}(t') \right)_\beta \left(\sum_{m''} c_{m''}^\dagger(t'') c_{m''}(t'') \right)_\gamma \right\rangle \eta_\beta \eta_\gamma \quad i = L, R \quad (9)$$

where the subscripts $+$, $\beta, \gamma = \pm$ refer to the positive (+) or negative (-) branch of the closed time path and $\eta_+ = +1$, $\eta_- = -1$ [12]. The time variable of a physical quantity (in our case the current) is always on the positive branch [12]. The coefficient $\alpha = C_G/C_\Sigma$. Next we perform a Fourier transformation and the result for the Fourier transform $I_i^{II}(\omega)$, $i = L, R$, is obtained in the form

$$I_i^{II}(\omega) = -2\pi e^3 \alpha^2 \int_{-\infty}^{\infty} d\omega' \text{Tr} \left\{ \left(\hat{\Sigma}_{ir}(\omega + \omega') - \hat{\Sigma}_{ia}(\omega') \right) \left[\hat{G}_r(\omega + \omega') \hat{G}_r(\omega' + \Omega) \hat{G}_<(\omega') \right. \right. \\ \left. \left. + \hat{G}_r(\omega + \omega') \hat{G}_<(\omega' + \Omega) \hat{G}_a(\omega') + \hat{G}_<(\omega + \omega') \hat{G}_a(\omega' + \Omega) \hat{G}_a(\omega') \right] \right. \\ \left. + \hat{\Sigma}_{i<}(\omega + \omega') \hat{G}_a(\omega + \omega') \hat{G}_a(\omega' + \Omega) \hat{G}_a(\omega') \right. \\ \left. - \hat{\Sigma}_{i<}(\omega') \hat{G}_r(\omega + \omega') \hat{G}_r(\omega' + \Omega) \hat{G}_r(\omega') \right\} \\ \times u_0^2 \left(\delta(\omega) + \delta(\omega - 2\Omega) \right) + \left(\Omega \rightarrow -\Omega \right). \quad (10)$$

Here $\hat{}$ above the symbol denotes a matrix in the level indices. The components of the matrix self-energies are defined in the following way:

$$\Sigma_{mm'iv} = \sum_k T_{imk} T_{im'k}^* A_{iv}(k, \omega) \quad (11)$$

where $v = r, a, <$ with $A_{iv}(k, \omega)$ being the retarded, advanced, and the distribution GF in the leads, respectively. The notation $(\Omega \rightarrow -\Omega)$ means that one adds the same terms as those explicitly written but with Ω replaced by $-\Omega$.

The terms with $\omega = 0$ in equation (10) contribute to the dc current through the dot. The coefficient of proportionality between the current and u_0^2 is defined as a rectification coefficient a_{rect} . The coefficient $a_{2\Omega}$ with $\omega = 2\Omega$ in equation (10) describes the amount of second-harmonic generation.

4. The nonlinear response of a dot with two degenerate levels

Let us consider the case of two degenerate levels $\epsilon_1 = \epsilon_2 = \epsilon$ ignoring all higher levels. The dot electrons GF are now diagonal and $G_{11} = G_{22} = G$. They are calculated using the method of irreducible Green's functions [14, 15]. The retarded Green's function for the dot electrons is obtained in the form

$$G_r = \frac{\omega - \tilde{\epsilon}_{-m} - \Sigma_0 - \Sigma_1}{(\omega - \epsilon_m - \Sigma_0)(\omega - \epsilon - \Sigma_0 - \Sigma_1) - E_c(\omega - \epsilon_m - \Sigma_0 - \Sigma_2)} \quad (12)$$

where the analytical continuation $\omega \rightarrow \omega + i0^+$ is used. The self-energy parts in equation (12) are given by

$$\Sigma_0(\omega) = \sum_{i=L,R} \Sigma_{0i}(\omega) \quad \Sigma_{0i}(\omega) = \sum_k \frac{|T_{ik}|^2}{\omega - \epsilon_{ik}} \quad (13)$$

$$\Sigma_1(\omega) = \sum_{k,i=L,R} |T_{ik}|^2 \left[\frac{1}{\omega - \epsilon_{-m} - \epsilon_m + \epsilon_{ik}} + \frac{1}{\omega + \epsilon_{-m} - \epsilon_m - \epsilon_{ik}} \right] \quad (14)$$

$$\Sigma_2(\omega) = \sum_{k,i=L,R} |T_{ik}|^2 f(\epsilon_{ik}) \left[\frac{1}{\omega + \epsilon_{-m} - \epsilon_m - \epsilon_{ik}} + \frac{1}{\omega - \epsilon_{-m} - \epsilon_m + \epsilon_{ik}} \right] \quad (15)$$

where $f(\epsilon_{ik})$, $i = L, R$, is the Fermi-Dirac distribution function for the electrons in the leads. We have used the following notation: $\epsilon_m = \epsilon + E_c \langle n_{-m} \rangle$ and $\tilde{\epsilon}_m = \epsilon + E_c (1 - \langle n_{-m} \rangle)$, where $\langle n_m \rangle$ is the average number of electrons on the level $m = 1, 2$, in the dot. The notation $-m$ is understood as $-1 = 2, -2 = 1$. We have omitted the subscript m in the tunnelling matrix elements since in the present case they do not depend on the level indices. The self-energies in equation (10) are now given by $\Sigma_{11i} = \Sigma_{22i} = \Sigma_{0i}$, $\Sigma_{12i} = \Sigma_{21i} = 0$.

The Green's function in equation (12) describes two levels for the quantum dot electrons—a lower (resonant) level with energy $\sim \epsilon$ and the upper level with energy $\sim \epsilon + E_c$. The relative weight of the lower/upper level in the density of states for the dot electrons is proportional to $1 - \langle n_{-m} \rangle / \langle n_{-m} \rangle$, respectively. We should point out that the Green's function presented here is valid for temperatures higher than the characteristic temperature for the problem—the Kondo temperature T_K . Lacroix [16] has shown that for temperatures $T < T_K$ this derivation procedure omits terms which are divergent at the Fermi level. These terms give rise to the Kondo effect. The exact noninteracting electron GF is obtained from equation (12) with $E_c = 0$.

The distribution Green's function is calculated under the assumption that the transient processes after switching on the dc bias have decayed, and the result is

$$G_<(\omega) = \frac{\Sigma_{0<}(\omega)}{(\Sigma_{0r}(\omega) - \Sigma_{0a}(\omega))} \left(G_r(\omega) - G_a(\omega) \right) \quad (16)$$

where

$$\Sigma_{0<}(\omega) = \sum_{k,i=L,R} |T_{ik}|^2 A_{i<}(\omega)$$

and $A_{i<}(\omega)$, $i = L, R$, is the distribution Green's function in the left-hand (right-hand) lead, respectively. The average number of electrons $n = \langle n_m \rangle = \langle n_{-m} \rangle$ is obtained by self-consistently solving the equation

$$n = \int \frac{d\omega}{2\pi} \text{Im } G_<(\omega). \quad (17)$$

In the following we discuss the nonlinear response of a quantum dot in the approximation of energy-independent tunnelling matrix elements. This means that we take the elastic level widths

$$\gamma_{L(R)}(\omega) = \pi \sum_k |T_{L(R)k}|^2 \delta(\omega - \epsilon_{L(R)k}) \quad (18)$$

to be constants $\gamma_{L(R)}$, independent of ω . The calculations are performed by taking a broad flat density of states for the lead electrons [16]. We take the band width in the leads to be much larger than E_c , eV , eV_G , and Ω . We must point out, however, that the static I – V characteristic which is obtained in this approach (the so-called Coulomb staircase) is a monotonically increasing function of V and does not have regions of negative differential resistance. The negative differential resistance appears when a dot electron energy level approaches the band edge in the leads and this is not possible in our approximation.

Now we present our numerical results for the rectification coefficient and the second-harmonic generation coefficient of a quantum dot. The numerical procedure is as follows. First, one solves equation (17) to obtain the average number of electrons in the dot and then computes a_{rect} and $a_{2\Omega}$ from equation (10). We have chosen the following values for the model parameters: $E_c = 100 \gamma$, $C_L = C_R = 5 \times 10^{-5} e^2/\gamma$, and $C_G = 10^{-5} e^2/\gamma$.

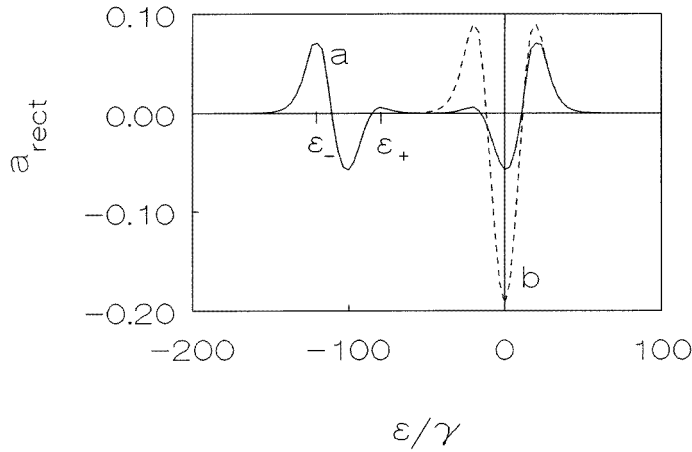


Figure 2. The rectification coefficient a_{rect} (in units of $e^3/\hbar\gamma$) versus the resonant level energy ϵ (relative to the right-hand chemical potential $\mu_R = 0$) for (a) interacting (solid line) and (b) noninteracting (dashed line) electrons. The frequency is $\Omega = 10\gamma$ and the dc voltage $eV = 20\gamma$.

In figure 2 we have plotted a_{rect} as a function of the position of the resonant level (relative to the right-hand chemical potential) of a dot, symmetrically coupled to the leads ($\gamma_L = \gamma_R$). The rectification coefficient for noninteracting electrons (figure 2, curve (b)) has a characteristic three-peak structure—one central (negative) and two side (positive) peaks. It is nonzero when the resonant level energy is in the vicinity of the right-hand chemical potential (μ_R is set to 0). In the case of interacting electrons (figure 2, curve (a)) there are two sets of peaks at energies close to 0 and $-E_c$ corresponding to the cases when the resonant or the upper level is near μ_R . The side peaks are not symmetric with respect to the negative one. The upper side peak (the peak at higher gate voltage) for the upper level and the lower side peak for the resonant level are suppressed. This is connected to the dependence of the relative weights of both levels in the density of states on the

average number of electrons in the dot. Consider the peaks corresponding to the upper level. Recall that the relative weight for the upper level is proportional to n . Each GF in the expression for a_{rect} (equation (10)) contributes a factor n ; thus, a_{rect} is proportional to n^3 in the vicinity of $\epsilon = -E_c$. The average number of dot electrons $2n$ decreases as the resonant level energy approaches the collector chemical potential since there are more and more states in the collector available for the tunnelling electron. The ratio of the height of the lower side peak (at $\epsilon = \epsilon_-$; see figure 2) to the height of the upper side peak (at $\epsilon = \epsilon_+$) is ~ 9.2 while the ratio $n^3(\epsilon_-)/n^3(\epsilon_+) \approx 7.6$. Hence, the dependence of the relative weight of the upper level on the resonant level energy explains reasonably well the heights of the side peaks. Of course, there are more factors influencing the heights of the peaks, e.g. the Fermi–Dirac distribution functions in equation (10) which lead to an additional suppression of the height of the upper side peak. We stress that this behaviour clearly results from the Coulomb blockade since in the noninteracting case the side peaks have equal heights. The ratio of the heights of the side peaks for the resonant level can be similarly explained. In this case the relative weight of the lower level is proportional to $1 - n$ and increases as the resonant level energy approaches μ_R .

Let us now discuss qualitatively the behaviour of a_{rect} when more than one resonant level is taken into account. Consider again the peaks of a_{rect} corresponding to the upper level. They appear when one electron from a quantum dot with N electrons (two in our case) can tunnel out of the dot leaving it in a state with $N - 1 \neq 0$ electrons (one electron in our case). Thus, for a dot with many levels the dependence of a_{rect} on the gate voltage will have the same qualitative behaviour as that for the upper level in the case that we have studied. The rectification coefficient will show the same structure of one central (negative) and two side (positive) peaks around the gate voltage at which one electron can tunnel out of the dot. The spacing between successive three-peak structures will be equal to the Coulomb charging energy, that is, the energy needed to add an electron to a quantum dot with N electrons. The heights of the side peaks will depend in some complicated way on the average number of electrons at every energy level in the dot. We can expect that in this case the suppression of the upper side peak height will be smaller since the relative change of the average number of dot electrons is smaller (one electron leaves a dot with 10–20 electrons).

The behaviour of a_{rect} as a function of the position of the resonant level (i.e. the gate voltage applied to the dot) that we have obtained is qualitatively similar to the recent experimental result of Kouwenhoven *et al* [17] on single-electron tunnelling through a quantum dot in the presence of microwave radiation. Kouwenhoven *et al* [17] analysed their results on the basis of the Tien–Gordon theory [18] of photon-assisted tunnelling. From this theory one would expect to find that the two side (positive) peaks are at a distance Ω from the central peak. This distance in our results is bigger than Ω . We attribute this behaviour to the effect of the temperature. The thermal fluctuations not only broaden the peaks but they also shift the positions of the peaks to higher energies or frequencies (see the discussion of the frequency dependence of a_{rect} below).

Let us now discuss the frequency behaviour of the rectification coefficient. The results are presented on figures 3 and 4. We consider two cases with different behaviours of a_{rect} . They are distinguished by the positions of the resonant level relative to that of the collector chemical potential. In figure 3 we show a_{rect} for noninteracting dot electrons calculated for the resonant level below the collector chemical potential, for $\epsilon = -200 \gamma$, for applied dc voltage $eV = 50 \gamma$ and for temperature $T = 0$ (curve (a)) and $T = 5 \gamma$ (curve (b)). At zero temperature a_{rect} is nonzero over a frequency interval with a width equal to the applied dc voltage. The maximum of a_{rect} appears at a frequency equal to the resonant

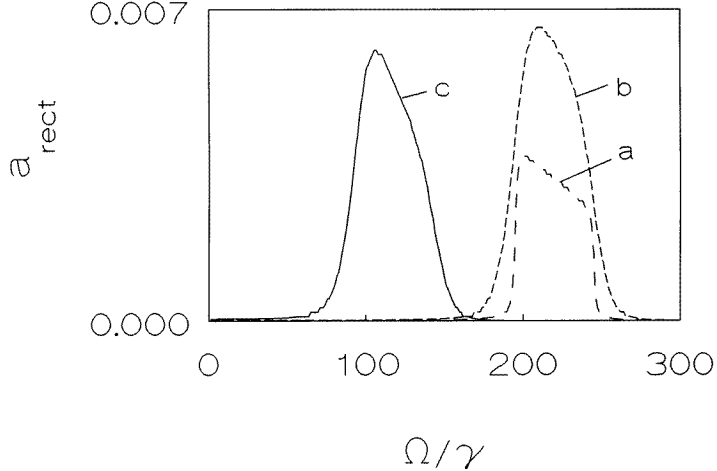


Figure 3. The rectification coefficient a_{rect} (in units of $e^3/\hbar\gamma$) versus the frequency of the applied ac field for noninteracting (curves (a) and (b)) and interacting dot electrons (curve (c)). The resonant level energy is $\epsilon = -200\gamma$ and the dc voltage $eV = 50\gamma$. The temperatures are $T = 0$ (curve (a)) and $T = 5\gamma$ (curves (b) and (c)). Note that the data for curves (a) and (b) have been multiplied by a factor of 4.

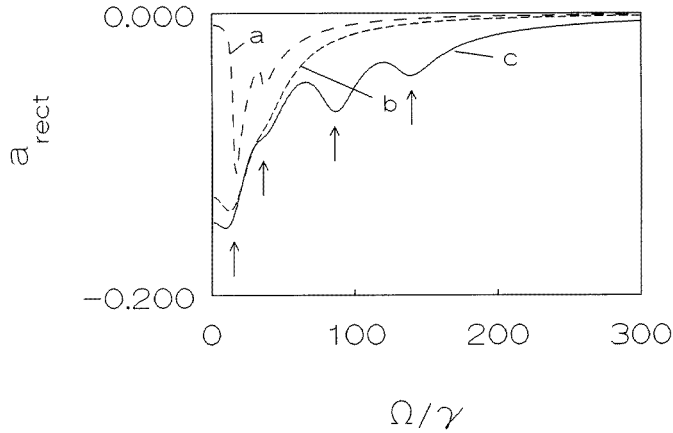


Figure 4. The rectification coefficient a_{rect} (in units of $e^3/\hbar\gamma$) versus the frequency of the applied ac field for noninteracting (curves (a) and (b)) and interacting dot electrons (curve (c)). The resonant level energy is $\epsilon = 35\gamma$ and the dc voltage $eV = 50\gamma$. The temperatures are $T = 0$ (curve (a)) and $T = 5\gamma$ (curves (b) and (c)). Note that the data for curve (c) have been multiplied by a factor of 4.

level energy (equation (2)). At nonzero temperature the peak of a_{rect} broadens and its maximum shifts to higher frequencies as compared to the $T = 0$ case. This feature arises as a result of the photon-assisted tunnelling. Since the resonant level is well below the collector chemical potential, there are no free-electron states in the collector available for the tunnelling electron. The electron must absorb a photon to tunnel through the right-hand barrier. When the Coulomb interaction is taken into account the dependence of a_{rect} on Ω

(figure 3, curve (c)) is similar to that in the case of noninteracting dot electrons that we have just discussed, with the exception that the maximum appears near the frequency $\Omega \sim \epsilon + E_c$. It is easy to understand this behaviour: since the resonant level is well below the collector chemical potential the average number of electrons in the dot is bigger than one—there is always one electron on the resonant level. In this case the transport through the dot occurs only through the upper level. The width of the frequency interval with nonzero values of a_{rect} is equal to eV because electrons in the left-hand lead (the emitter) with energies between μ_R and μ_L can tunnel through the dot.

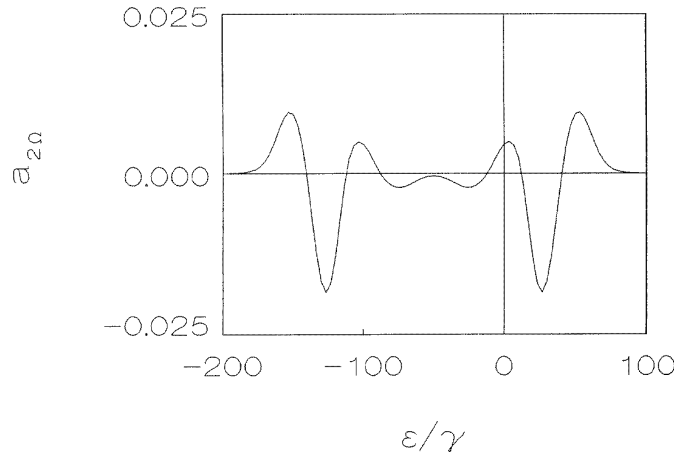


Figure 5. The second-harmonic generation coefficient $a_{2\Omega}$ (in units of $e^3/\hbar\gamma$) versus the resonant level energy ϵ for interacting dot electrons. The dc voltage is $eV = 20\gamma$ and the temperature is $T = 5\gamma$.

In figure 4 we present the frequency dependence of a_{rect} for a quantum dot in the case where the resonant level energy is above the collector chemical potential. The calculation is performed for the following set of parameters: $\epsilon = 35\gamma$ and $eV = 50\gamma$. We consider two cases for noninteracting electrons in which the temperature is $T = 0$ (curve (a)) and $T = 5\gamma$ (curve (b)). The results for the interacting case are presented in figure 4 (curve (c)) for $T = 5\gamma$. At zero temperature (curve (a)) a_{rect} displays a resonant behaviour with two sharp peaks at frequencies $\Omega = |\epsilon - \mu_L|$ and $\Omega = |\epsilon - \mu_R|$ (recall that we have set $\mu_L = eV$ and $\mu_R = 0$). At higher temperatures the second peak is almost smeared out by the thermal fluctuations (curve (b)). The rectification coefficient for interacting electrons has four features (peaks) near the frequencies (figure 4, curve (c); the peaks are marked with arrows for increasing values of Ω) $\Omega = |\epsilon - \mu_L|$, $\Omega = |\epsilon - \mu_R|$, $\Omega = |\epsilon + E_c - \mu_L|$, and $\Omega = |\epsilon + E_c - \mu_R|$. The first two peaks come from the lower (resonant) level (they coincide with the corresponding features in the noninteracting case) and the latter two are from the upper level. In the case that we are considering, the upper level (at energy $\sim \epsilon + E_c = 135\gamma$) is above the emitter chemical potential $\mu_L = eV = 50\gamma$. The dc tunnelling current from the emitter to the collector flows only through the resonant level—the upper level is not occupied (there are no available electrons in the emitter at energy $\epsilon + E_c$ that can tunnel to the dot). In a time-dependent field the peaks in the frequency dependence of a_{rect} are a demonstration of the photon-assisted tunnelling—the electron must absorb a photon to jump to the upper level in order to tunnel through the left-hand barrier.

We now compare our results for the frequency dependence of a_{rect} to the results reported by Frensel [9]. Frensel computed the Wigner function of the dot in the presence of a time-dependent potential taking into account the effect of all resonant levels in the dot. He obtained resonant enhancement of the rectification coefficient in the frequency range 1–8 THz. However, the distance between the lowest resonant levels was much larger than the frequency of the applied ac field which rules out photon-assisted transitions between these levels. The results of Frensel [9] and our work suggest that the resonant-like enhancement of the rectification coefficient is not due to the transitions between different resonant levels in the dot. It results from the photon-assisted tunnelling through the dot.

Now we briefly discuss the behaviour of the second-harmonic generation coefficient. For relatively small driving frequencies it has qualitatively the same gate voltage dependence as a_{rect} . Obviously, the two coefficients coincide for zero driving frequency:

$$a_{rect}(\Omega = 0) = a_{2\Omega}(\Omega = 0) = \frac{d^2 I}{dV^2} \quad (19)$$

where $I(V)$ is the dc current–voltage characteristic of the dot. For higher frequencies the peaks in the gate voltage dependence of $a_{2\Omega}$ are significantly displaced compared to the peaks of a_{rect} due to the different frequency arguments of the Green's functions in equation (10). In figure 5 we present the gate voltage dependence of $a_{2\Omega}$ calculated for the following parameter values: $eV = 20\gamma$, $T = 5\gamma$, and $\Omega = 25\gamma$. Note the peak displacement equal to the driving frequency.

5. Discussion

In this section we address the applicability of the approach that we have adopted to experiments. We have considered the lead electrons as noninteracting particles. In real systems, electrons near the quantum dot barriers contribute to the self-consistent potential. Thus, one should (1) self-consistently determine the tunnelling matrix elements and single-particle energies, and (2) calculate the transport characteristics of a system with these self-consistent parameters. In this work we consider only step (2) assuming the results of (1) as input parameters. The on-site repulsion energy can be estimated from $E_c \sim e^2/\epsilon L$, where L is the size of the confined region, and ϵ is the dielectric constant for the GaAs. Thus for a quantum dot with an average size of 100 Å, one gets $E_c \sim 1\text{--}10$ meV. It is less evident how to estimate the elastic broadening constant γ , but we can use the estimation given in [19] for $\gamma \sim 10\text{--}20$ μeV for a structure of about the same size. We must point out that our calculation takes into account only the level width which is due to tunnelling (the self-energies in equations (13)–(15)). There are other mechanisms which broaden the level and they lead to some new renormalized level width which may be much larger than γ . The approach in this work in the interacting case is limited to the following range of the main parameters in the model: $E_c \gg T \gg \gamma$. In the case of noninteracting electrons we used a phenomenological model where the total level width is expressed as a sum of elastic and inelastic widths, $\gamma = \gamma_{el} + \gamma_{inel}$. The nonlinear response coefficients showed the same characteristic sets of peaks which were suppressed in height and additionally broadened [20].

We modelled the electron–electron Coulomb interaction by an impurity Anderson model i.e. we considered only the on-site part of the interactions. By neglecting the long-range interactions, we do not describe correlations between charge fluctuations at different sites of the system. Recently, Büttiker and co-workers [21] emphasized the importance of the long-range interactions in mesoscopic systems. We must point out in this context that the current is conserved in our model: $I_L^{tot} + I_R^{tot} + I_G = 0$, where $I_{L/R}^{tot}$ is the current through

the left/right-hand barrier (equation (8)) and I_G is the capacitive gate electrode current. This current conservation results from the long-range nature of the Coulomb interactions. On the other hand, the impurity Anderson model has all of the features necessary to describe the Coulomb blockade in a quantum dot. Thus, we believe that our approach correctly describes the nonlinear response of the dot in most of the experimental situations for driving frequencies that are not too high. The frequency of the external ac bias must be smaller than the plasma frequency of the leads. The plasma frequency is of the order of tens of THz; this value is well above the present experimentally accessible frequencies, ~ 5 THz.

In conclusion, we have calculated the nonlinear response coefficients (the rectification coefficient and the second-harmonic generation coefficient) of a quantum dot with interacting electrons. As functions of the position of the resonant level they have two characteristic sets of peaks reflecting the energy spectrum of the electrons. The heights of the peaks are consistent with the dependence of the relative weight of the two levels in the density of states on the average number of electrons in the dot—a feature which is a direct consequence of the electron interactions. The frequency dependence of the rectification coefficient shows clear evidence of a photon-assisted tunnelling—the electron absorbs a photon to tunnel through a barrier. The resonant-like enhancement of the rectification coefficient is not due to the photon-induced transitions between different resonant levels in the dot since it appears when there is only one resonant level in the dot.

Acknowledgments

The author acknowledges fruitful discussions with Dr V Valtchinov. The work was sponsored by Contract F-522 with the National Foundation for Scientific Research of Bulgaria.

References

- [1] Ozbay E, Diamond S K and Bloom D M 1990 *Electron. Lett.* **26** 1046
- [2] Brown E R, Goodhue W D and Sollner T C L G 1988 *J. Appl. Phys.* **64** 1519
Brown E R, Sollner T C L G, Parker C R, Goodhue W D and Cheng C L 1989 *Appl. Phys. Lett.* **55** 1777
- [3] Brown E R, Soderstrom J R, Parker C D, Mahoney L J, Molvar K M and McGill T C 1991 *Appl. Phys. Lett.* **58** 2291
- [4] Sollner T C L G, Goodhue W D, Tannewald P E, Parker C D and Peck D D 1983 *Appl. Phys. Lett.* **43** 588
- [5] Chen L Y and Ting C S 1990 *Phys. Rev. Lett.* **64** 3159; 1991 *Phys. Rev. B* **43** 2097
- [6] Ivanov T, Valtchinov V and Wille L T 1994 *Phys. Rev. B* **50** 4917
- [7] Fu Y and Dudley S C 1993 *Phys. Rev. Lett.* **70** 65
- [8] Bruder C and Schoeller H 1994 *Phys. Rev. Lett.* **72** 1076
- [9] Frenksley W R 1987 *Appl. Phys. Lett.* **51** 448; 1990 *Rev. Mod. Phys.* **62** 745
- [10] Wingreen N S 1990 *Appl. Phys. Lett.* **56** 253
- [11] Chitta V A, Kutter C, de Bekker R E M, Maan J C, Hawksworth S J, Chamberlain J M, Henini M and Hills G 1994 *J. Phys.: Condens. Matter* **6** 3945
- [12] Chow K C, Su Z B, Hao B L and Lu Yu 1985 *Phys. Rep.* **118** 1
- [13] Landau L D and Lifshitz E M 1981 *Physical Kinetics* (Oxford: Pergamon) ch X
- [14] Ivanov T, Marvakov D, Valtchinov V and Wille L T 1993 *Phys. Rev. B* **48** 4679
- [15] Tyablikov S B 1975 *Metodi Kvantovoi Teorii Magnetizma* (Moscow: Nauka)
- [16] Lacroix C 1981 *J. Phys. F: Met. Phys.* **11** 2389
- [17] Kouwenhoven L P, Jauhar S, McCormick K, Dixon D, McEuen P L, Nazarov Yu, van der Vaart N C and Foxon C T 1994 *Phys. Rev. B* **50** 2019
- [18] Tien P K and Gordon J R 1963 *Phys. Rev.* **129** 647
- [19] Foxman E, McEuen P, Meirav U, Wingreen N, Meir Y, Belk P, Kastner M and Wind S 1993 *Phys. Rev. B* **47** 10020
- [20] Ivanov T 1995 unpublished

[21] Büttiker M 1993 *J. Phys.: Condens. Matter* **5** 9361
Büttiker M, Thomas H and Pretre A 1993 *Phys. Lett.* **180A** 364